

EFFECT OF HOT ROLLING ON MICROSTRUCTURE AND TENSILE PROPERTIES OF Ti-Nb-Zr-Ta-O ALLOY

PREISLER Dalibor, STRÁSKÝ Josef, HARCUBA Petr, JANEČEK Miloš

*Charles University in Prague, Faculty of Mathematics and Physics, Department of Physics of Materials,
Prague, Czech Republic, EU*

preisler.dalibor@gmail.com, josef.strasky@gmail.com, harcuba.p@seznam.cz, janecek@met.mff.cuni.cz

Abstract

Biocompatible β -titanium alloy Ti-35.3Nb-7.3Zr-5.7Ta-0.7O (wt.%) shows high strength and reduced elastic modulus when compared to commercial alloys for total joint endoprostheses (e.g. Ti-6Al-4V). However, in the as-cast condition, porosity, dendritic chemical inhomogeneities and coarse grain structure negatively influence mechanical properties and therefore sequential thermo-mechanical treatment is necessary. Studied material (as-cast rod) was processed by hot rolling at 1200°C and three conditions with different diameter reduction were prepared. Scanning electron microscopy (SEM) along with electron back-scatter diffraction (EBSD) was employed to characterize resulting microstructure. Tensile tests and microhardness measurements were used to evaluate room temperature mechanical properties. SEM showed that porosity is removed by hot rolling and EBSD revealed deformed grain structure that is partially recrystallized in the center of each rod. There is a clear difference between the grain sizes of the three states in the center of rods. Yield strength exceeding 1050 MPa, ultimate tensile strength of values over 1200 MPa and plastic elongation > 20% in all three studied conditions indicate that hot-rolled Ti-35.3Nb-7.3Zr-5.7Ta-0.7O alloy can be used for implant manufacturing.

Keywords: Beta titanium, EBSD, deformation, recrystallization

1. INTRODUCTION

Titanium alloys find their use in various fields. An extraordinary combination of properties, such as excellent corrosion resistance, desirable biocompatibility and suitable mechanical properties, predetermine use of these alloys in orthopaedics [1, 2]. The most commonly used Ti alloy in orthopaedics is the $\alpha+\beta$ alloy Ti-6Al-4V, developed originally for aerospace industry. Its yield strength ranges from 850 MPa to 1050 MPa, depending on the processing route and α/β phase morphology. The drawback of Ti-6Al-4V alloy in medicine is however its content of toxic vanadium. By replacing of vanadium with suitable amount of niobium, this problem can be resolved and therefore Ti-6Al-7Nb alloy emerged [3]. Another issue is content of aluminium, whose possible neurodegenerative impact has not been settled yet. It is therefore suggested to employ only proven biocompatible elements [4]. Finally, all $\alpha+\beta$ alloys are characterized by Young's modulus of around 115 GPa that, although half than those of steels (200 GPa), is still 4 - 5 times higher than Young's modulus of cortical bone (20 GPa - 30 GPa). This incompatibility induces the so-called stress shielding effect (the implant material absorbs most of the load normally applied to bone) and consequent osteoporosis lowers the durability of an implant.

Current research focuses on development of β -Ti alloys with sufficient content of β -stabilizing elements to retain pure β phase after quenching from β region [5]. Pure β phase composition can lead to lower Young's moduli when compared to $\alpha+\beta$ alloys. Biocompatible alloy Ti-35.3Nb-7.3Zr-5.7Ta (wt.%) was designed using only biocompatible elements resulting in low Young's modulus. However, its yield strength (around 550 MPa) is not sufficient for the manufacturing of implants of big joints [6 - 8]. Adding small content of interstitial oxygen can considerably improve strength of alloy of this type [9 - 11]. Alloy Ti-35.3Nb-7.3Zr-5.7Ta-0.7O (wt.%) shows Young's modulus of 80 GPa and significantly improved strength [11, 12]. The as-cast alloy, however, contains micro-sized pores, very coarse grain structure and dendritic chemical inhomogeneities which results in

decreased strength [13] and presumably reduced fatigue performance. Subsequent thermomechanical treatment is therefore needed.

The effect of hot-rolling is investigated in the present study to simulate industrial processing of the Ti-35.3Nb-7.3Zr-5.7Ta-0.7O (wt.%) alloy.

2. EXPERIMENTAL

Initial rod of studied alloy (55 mm in diameter) was produced by Retech, Co., USA, by plasma arc melting of pure elements (and TiO₂ for the oxygen addition) into small compacts followed by sequential pour melting procedure in clean He atmosphere. Hot rolling of as-cast rod was performed at VŠB TU Ostrava, Czech Republic, and final rods of diameters 33 mm, 25 mm and 20 mm were produced by the following procedure. Two parts of initial rod were heated up to 1200 °C in air for more than 1 h and rolled to diameter of 33 mm by several rolling passes without reheating. The rod was rotated by 90° after each pass. One of the rods was reheated back to 1200 °C and rolled to diameter 25 mm by the same procedure. This rod was cut into two pieces and one of them was again heated back to 1200 °C and rolled to diameter 20 mm. After the last rod was finished, all three final pieces were cooled in water. Due to the rolling procedure, each rod was not exactly round but was wider in one direction (transverse direction of the corresponding last rolling step - this is the direction at which the diameter is measured) and this allows us to name the positions of samples according to **Figure 1** (C - center, T - transversal edge, N - normal edge). The other diameter (in the normal direction) was 25 mm, 22 mm and 18 mm for the rods with transverse diameter 33 mm, 25 mm and 20 mm, respectively. Each sample will be referred to as by its position and the transversal diameter of the corresponding rod (e.g. C33).

Samples for scanning electron microscopy (SEM) and electron back-scatter diffraction (EBSD) were ground with SiC papers up to 2400 grit. Three step polishing was done using Buehler vibratory polisher with Alumina 0.3 µm, Alumina 0.05 µm and Colloidal Silica 0.05 µm suspensions, 9 h for the first two steps and 3 h for the last step. SEM Quanta 200FX with FEG emitter operating at 10 kV and EDAX EBSD detector was used to microstructural characterization. Microhardness was measured on samples after SEM and EBSD observations using Vickers method (with load of 0.5 kgf) on Qness 10A+ hardness tester. Samples for tensile testing were cut from the rods in the rolling direction with the gauge length of 15 mm and the diameter of 3 mm. Room temperature tensile tests were performed on Instron 5882 machine at the strain rate 10⁻⁴ s⁻¹.

3. RESULTS AND DISCUSSION

SEM observations revealed that porosity present in the as-cast material is removed already in the least deformed condition (diameter 33 mm) as is shown in **Figure 2**. This figure also shows heavily deformed microstructure in which it is difficult to distinguish individual grains and EBSD method needs to be employed.

EBSD measurements were taken with the step size of 6 µm and results are shown in **Figures 3** and **4** employing grain orientation spread (GOS) maps. GOS is a characteristic angle for every grain and is calculated as an average misorientation of measured points in single grain and their mean orientation. Color scale of both the GOS's and grain boundary misorientations is shown in **Figure 5**. GOS maps in **Figure 3** show the central parts of the three rods (C33, C25 and C20). Increased deformation by rolling clearly causes progressive grain refinement. Also we can observe growing fraction of blue colored small grains that have low GOS values below 1° (4 % for C33, 11 % for C25 and 18 % for C20). Values of GOS below approx. 1° are characteristic for discontinuously recrystallized grains in β-Ti alloys [14]. We can therefore argue that the fraction of recrystallized grains in the central part rises with increasing deformation.

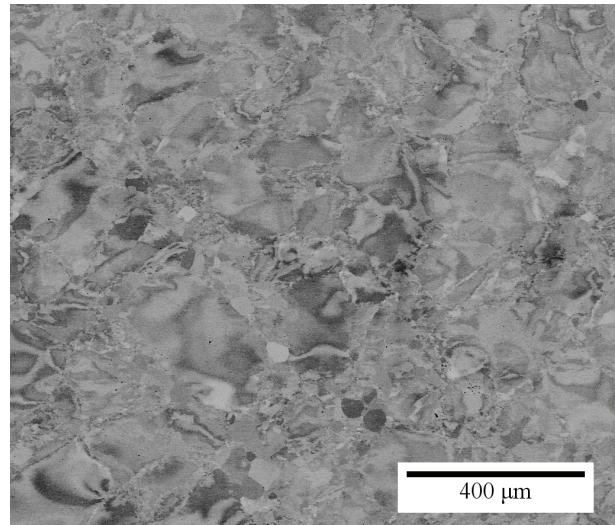
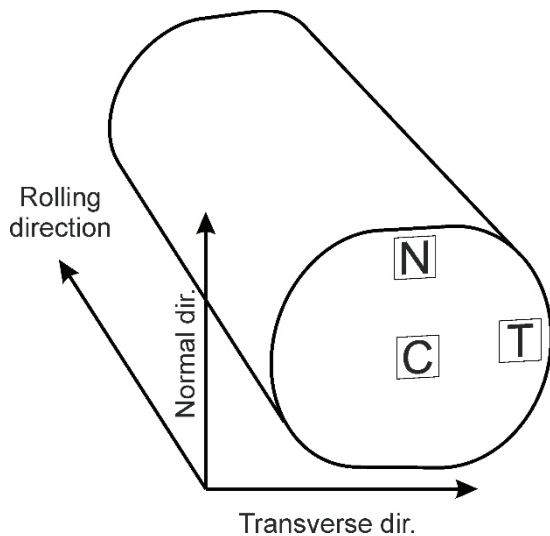


Figure 1 Graphic representation of sample positions

Figure 2 SEM image of rod with diameter 33 mm

GOS maps from the normal edges of the rolled rods (N33, N25 and N20) are shown in **Figure 4** (the transverse edges - not shown - are very similar to the normal edges). Unlike the central parts there is a negligible fraction of recrystallized grains (less than 2 % in all conditions). Grain refinement is less evident in the transverse edges. On the other hand, an increasing amount of low-angle grain boundaries and an increasing deformation within grains (more red and orange grains) is observed with increasing degree of rolling (diameter reduction).

The principal difference of absence of recrystallized grains in edges of rods can have a reason in lower degree of deformation and in lower temperature when compared to central parts. Higher deformation in the central parts compared to edges was found by finite elements method modelling for a similar rolling process of a magnesium alloy AZ31 [15]. Furthermore, the central parts of the three rods remained very hot throughout the process due to low thermal conductivity of titanium but the edges were cooled both by contact with the rolls and by surrounding air so the rods needed to be reheated. These conditions led to discontinuous recrystallization in the central parts while the edges could undergo only recovery processes which were recently found to take place in β -Ti alloys deformed at lower temperatures (820 °C - 900 °C) [14]. Partly recovered dislocation structure can be seen in all present GOS maps as low-angle grain boundaries. It appears that annealing at temperatures around 1200 °C could refine the deformed grains by discontinuous recrystallization but further experiments need to be performed to verify this hypothesis.

In **Table 1**, the results of microhardness measurements are shown. All differences in values are within the statistical error (standard deviation) although central parts seem to exhibit slightly higher hardness, as well as the normal edges compared to transverse edges in the more deformed states. Microstructural changes of the central parts also did not significantly affect the microhardness. However, in comparison with the microhardness of the as-cast state, 326 ± 6 HV [13], the microhardness in rolled material is clearly improved.

Tensile properties were improved by rolling for all conditions as documented by representative flow curves of rolled and as-cast material in **Figure 6**. Sharp yield point is present due to interaction of Cottrell atmospheres of interstitial oxygen atoms with the dislocations [16, 17] and is more pronounced in rolled material, arguably due to higher dislocation density induced through deformation. After short period of softening, an apparent strain hardening occurs until formation of a neck and a ductile fracture. In contrast, in the as-cast state, the brittle fracture is observed. Visible rise of the slope in rolled states (compared to as-cast state) in the elastic region is probably caused by different stiffness of fixing mechanisms used in the testing machine rather than increase in Young's modulus.

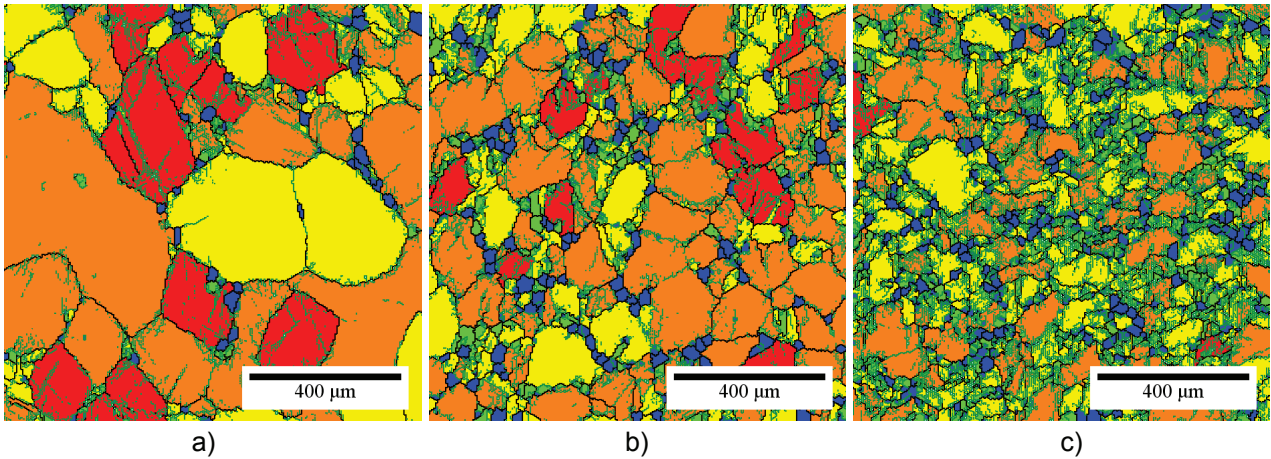


Figure 3 GOS maps of central parts of rods with diameter a) 33 mm, b) 25 mm, c) 20 mm

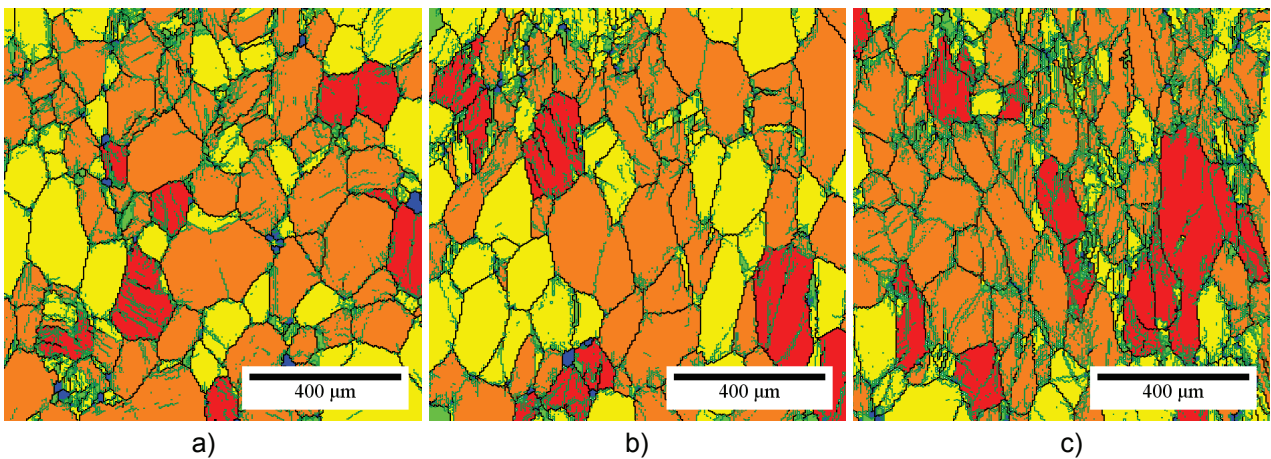
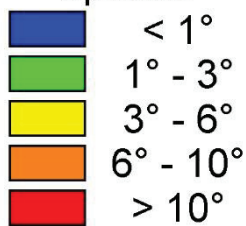


Figure 4 GOS maps of normal edges of rods with diameter a) 33 mm, b) 25 mm, c) 20 mm

Grain orientation spread:



Grain boundary misorientation:

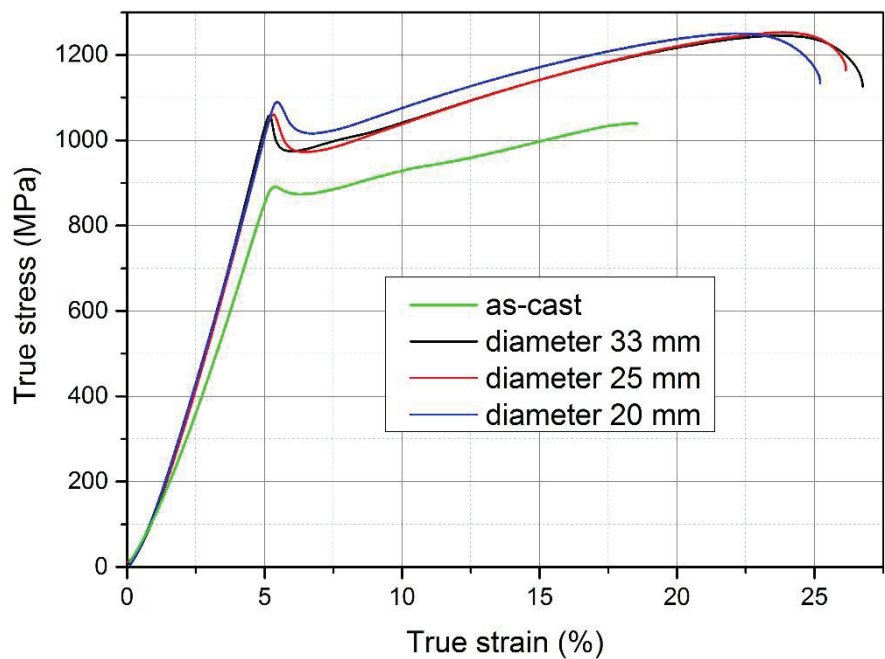
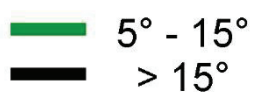


Figure 5 Legend for GOS maps

Figure 6 Stress - strain curves for as-cast [13] and rolled material

Table 1 Microhardness measurements of different rods / positions (HV 0.5)

↓Diameter / position→	C (center)	N (normal edge)	T (transverse edge)
33 mm	343 ± 5	339 ± 7	338 ± 5
25 mm	344 ± 7	342 ± 6	336 ± 6
20 mm	345 ± 7	346 ± 4	335 ± 6

Table 2 Tensile properties of rolled material

Rod diameter	Yield strength (MPa)	Ultimate tensile strength (MPa)	Elongation (%)
33 mm	1053 ± 4	1251 ± 4	21.9 ± 0.3
25 mm	1078 ± 14	1256 ± 6	20.9 ± 1.2
20 mm	1084 ± 7	1237 ± 19	20.0 ± 1.2

Yield strength, ultimate tensile strength and elongation (true plastic strain at fracture) values of rolled rods are shown in **Table 2**. Each value is computed from 3 measured samples. Yield strength clearly increases with the reduction of final diameter, while elongation decreases insignificantly and still reaches 20%. Ultimate tensile strength remains the same within the statistical error in all three rolled states.

Tensile properties of the rolled material are superior to those of commercial (and mostly used) Ti-6Al-4V alloy. Moreover, the studied alloy consists only of biocompatible elements and has lower Young's modulus. Rolled Ti-35.3Nb-7.3Zr-5.7Ta-0.7O alloy can be readily used to hip implants manufacturing.

4. CONCLUSION

- Alloy Ti-35.3Nb-7.3Zr-5.7Ta-0.7O (wt.%) was processed by hot rolling at 1200 °C after casting.
- Porosity is removed by hot rolling and heavily deformed microstructure is introduced. The microstructure is partly recrystallized in the center of the rods due to higher deformation and longer exposure to higher temperatures. Recrystallization does not occur on the edges where the material is less deformed and cools faster.
- Tensile properties are greatly improved after processing. In all prepared conditions, yield strength exceeds 1050 MPa and elongation > 20% is obtained. Sharp yield point is more pronounced in hot-rolled alloy due to higher dislocation density interacting with interstitial oxygen.
- Hot-rolled Ti-35.3Nb-7.3Zr-5.7Ta-0.7O biocompatible alloy shows superior properties to Ti-6Al-4V and can be used for implant manufacturing.

ACKNOWLEDGEMENTS

Financial support by the Czech Science Foundation (grant No. 17-20700Y) and by the Grant Agency of Charles University (project GAUK No. 1530217) is gratefully acknowledged.

REFERENCES

- [1] RACK, H. J., QAZI, J. I. Titanium alloys for biomedical applications. *Materials Science and Engineering: C*, 2006, vol. 26, no. 8, pp. 1269-1277.
- [2] GEETHA, M., SINGH, A. K., ASOKAMANI, R., GOGIA, A.K. Ti based biomaterials, the ultimate choice for orthopaedic implants - A review. *Progress in Materials Science*, 2009, vol. 54, pp. 397-425.
- [3] SEMLITSCH, M., STAUB, F., WEBER, H. Titanium-aluminium-niobium alloy, development for biocompatible, high strength surgical implants. *Biomedical Engineering*, 1985, vol. 30, no. 12, pp. 334-339.

- [4] EISENBARTH, E., VELTEN, D., MÜLLER, M., THULL, R., BREME, J. Biocompatibility of β -stabilizing elements of titanium alloys. *Biomaterials*, 2004, vol. 25, no. 26, pp. 5705-5713.
- [5] NIINOMI, M. Mechanical biocompatibilities of titanium alloys for biomedical applications, *Journal of the Mechanical Behavior of Biomedical Materials*, 2008, vol. 1, no. 1, pp. 30-42.
- [6] AHMED, T., RACK, H. J. *Low modulus biocompatible titanium base alloys for medical devices*. U.S. Patent No. 5,871,595, 1999.
- [7] FERRANDINI, P. L., CARDOSO, F. F., SOUZA, S. A., AFONSO, C. R., CARAM, R. Aging response of the Ti-35Nb-7Zr-5Ta and Ti-35Nb-7Ta alloys. *Journal of Alloys and Compounds*, 2007, vol. 433, no. 1-2, pp. 207-210.
- [8] ELIAS, L. M., SCHNEIDER, S. G., SCHNEIDER, S., SILVA, H. M., MALVISI, F. Microstructural and mechanical characterization of biomedical Ti-Nb-Zr (-Ta) alloys. *Materials Science and Engineering: A*, 2006, vol. 432, no. 1, pp. 108-112.
- [9] BESSE, M., CASTANY, P., GLORANT, T. Mechanisms of deformation in gum metal TNTZ-O and TNTZ titanium alloys: A comparative study on the oxygen influence. *Acta Materialia*, 2011, vol. 59, no. 15, pp. 5982-5988.
- [10] QAZI, J. I., RACK H. J., MARQUARDT B. High-strength metastable beta-titanium alloys for biomedical applications. *Journal of Materials Science*, 2004, vol. 56, no. 11, pp. 49-51.
- [11] STRÁSKÝ, J., HARCUBA, P., VÁCLAVOVÁ, K., HORVÁTH, K., LANDA, M., SRBA, O., JANEČEK, M. Increasing strength of a biomedical Ti-Nb-Ta-Zr alloy by alloying with Fe, Si and O. *Journal of the Mechanical Behavior of Biomedical Materials*, 2017, vol. 71, pp. 329-336.
- [12] STRÁSKÝ, J., JANEČEK, M., HARCUBA, P., LANDA, M. Increasing strength of Ti-Nb-Zr-Ta biomedical alloy via oxygen content. In *METAL 2014: 23rd International Conference on Metallurgy and Materials*. Ostrava: TANGER, 2014, pp. 1127-1132.
- [13] PREISLER, D., VÁCLAVOVÁ, K., STRÁSKÝ, J., JANEČEK, M., HARCUBA, P. Microstructure and mechanical properties of Ti-Nb-Zr-Ta-O biomedical alloy. In *METAL 2016: 25rd International Conference on Metallurgy and Materials*. Ostrava: TANGER, 2016, pp. 1509-1513.
- [14] ZHAO, J., ZHONG, J., YAN, F., CHAI, F., DARGUSCH, M. Deformation behaviour and mechanisms during hot compression at supertransus temperatures in Ti-10V-2Fe-3Al. *Journal of Alloys and Compounds*, 2017, vol. 710, pp. 616-627.
- [15] STEFANIK, A., SZOTA, P., MRÓZ, S., BAJOR, T., BOCZKAL, S. Influence of deformation method on the microstructure changes in AZ31 magnesium alloy round rods obtained by the rolling process. *Key Engineering Materials*, 2016, vol. 716, pp. 864-870.
- [16] COTTRELL, A. H., BILBY B. A. Dislocation theory of yielding and strain ageing of iron. *Proceedings of the Physical Society. Section A*, 1949, vol. 62, no. 1, pp. 49-62.
- [17] GENG, F., NIINOMI, M., NAKAI, M. Observation of yielding and strain hardening in a titanium alloy having high oxygen content. *Materials Science and Engineering: A*, 2011, vol. 528, no. 16, pp. 5435-5445.